

How brain corals record climate: an integration of skeletal structure, growth and chemistry of *Diploria labyrinthiformis* from Bermuda

Anne L. Cohen¹, Struan R. Smith², Michael S. McCartney¹, Jackie van Etten³

¹Woods Hole Oceanographic Institution, Woods Hole, Massachusetts 02543, USA

²Bermuda Biological Station for Research, Ferry Reach, St. Georges GE01, Bermuda

³Bridgewater State College, Bridgewater, Massachusetts 02325, USA

ABSTRACT: The aragonite skeleton of massive reef-building corals contains a record of the oceanic environment in which they grow. However, reading of the record requires understanding of how it is archived, a process complicated by the elaborate skeletal construction and seasonal growth patterns that characterize many species. In this study, we assess the utility of the massive brain coral *Diploria labyrinthiformis* as an archive of sea surface temperature (SST) variability in the western North Atlantic. *In situ* staining of live colonies combined with microscale analysis of skeletal chemistry indicate that *D. labyrinthiformis* grows throughout the year on Bermuda and records the full annual cycle of SST variability. However, skeleton accreted during the summer is overlain (thickened) by skeleton accreted during the subsequent fall and winter. As a result, conventional coarse sampling for $\delta^{18}\text{O}$ enables seasonal $\delta^{18}\text{O}$ cycles to be resolved but these do not capture the full amplitude of the annual SST cycle. Our data show that the shallow gradient of the $\delta^{18}\text{O}$ -SST regression equation derived for *D. labyrinthiformis* ($-0.113\text{‰ }^{\circ}\text{C}^{-1}$) relative to the expected $-0.22\text{‰ }^{\circ}\text{C}^{-1}$ for marine skeletons results from dampening of the summertime peak in $\delta^{18}\text{O}$. In contrast, skeleton accreted during the winter is not thickened and wintertime $\delta^{18}\text{O}$ captures the interannual wintertime SST variability at this site. Using SIMS ion microprobe to analyse strontium to calcium ratios (Sr/Ca), we avoided the thickening deposits and were able to resolve the full amplitude of the annual Sr/Ca cycle. The Sr/Ca-SST relationship obtained for *D. labyrinthiformis* ($-0.0843 \text{ mmol/mol }^{\circ}\text{C}^{-1}$) corresponds to that derived from fast-growing tropical reef corals. X-ray intensity ratios, used as a proxy for skeletal density, reveal the expected seasonal changes associated with growth banding as well as variability on inter-annual and decadal timescales. These variations are well correlated with wintertime SST variability in the subtropical gyre and may be a valuable proxy thermometer for the North Atlantic.

KEY WORDS: North Atlantic · Sea surface temperature · Coral · Stable isotopes · Sr/Ca · Density bands

Resale or republication not permitted without written consent of the publisher

INTRODUCTION

Knowledge of how the ocean behaves on decadal and longer timescales depends to a large extent on proxy records constructed from information stored in the skeletons of marine organisms. Of the enormous variety of biologic archives in the marine environment, massive reef corals are uniquely suited to provide highly resolved, continuous records of surface ocean variability over the past several hundred years (Cole & Dunbar 1999, Gagan et al. 2000). The majority of coral-based climate records thus far constructed have been for the

equatorial Pacific where the magnitude of interannual temperature anomalies associated with El Niño-Southern Oscillation (ENSO) events far exceeds that of the seasonal sea surface temperature (SST) cycle (e.g. Cole et al. 1993, Quinn et al. 1998, Urban et al. 2000). Here, massive corals of the genus *Porites* are abundant, long-lived and fast-growing, and are particularly suited to providing long, seasonally resolved time series of ocean variability. By comparison, reconstruction of high-resolution proxy records of mid-latitude SST variability is challenging because low-amplitude interannual variability may be masked by

the large seasonal cycle. For example, SSTs on the Bermuda platform fluctuate seasonally over a range of 10°C while the year-to-year variations associated with regional climate changes are typically less than 1°C (Joyce & Robbins 1996). Furthermore, the slow growth rates of many subtropical species and varying degrees of skeletal thickening may limit the temporal resolution of proxy records obtained using the conventional coarse (i.e. non-microbeam) sampling techniques (Barnes et al. 1995).

In this study, we assessed the potential of the massive brain coral *Diploria labyrinthiformis* to provide proxy records of wintertime SST variability in the subtropical North Atlantic. Our interest in the wintertime surface ocean was its relation to the North Atlantic Oscillation (NAO), a major source of winter climate variability in the Atlantic sector (Hurrell 1995). Whilst the NAO is an atmospheric phenomenon, its variability is reflected in wintertime SSTs of the mid- to high-latitude North Atlantic, on interannual through multi-decadal timescales (Fig. 1) (Bjerknes 1964, Molinari et al. 1997, Visbeck et al. 2001). The position of Bermuda (64°W, 32°N) in the North Atlantic subtropical gyre is well suited to index SST variability associated with NAO. Local wintertime sea surface temperature anomalies (SSTAs) are correlated with NAO since 1955 (Fig. 1) and reflect the larger-scale SSTA variability of the western North Atlantic (Joyce & Robbins 1996, Talley 1996). Despite its slow growth rate (less than one half of Pacific *Porites* spp.) and complex skeletal architecture, we targeted *D. labyrinthiformis* as a potential archive of paleoSST because of its abundance on Bermuda and throughout the Caribbean, its tendency to build massive, long-lived

colonies, and the presence of strong annual growth bands in the skeleton (Logan & Tomascik 1991, 1994, Dodge & Thompson 1974). We compared chemical (oxygen isotope ratios, $\delta^{18}\text{O}$; strontium to calcium ratios, Sr/Ca) and structural (density) variability in the skeletons of live colonies with instrumental data from Bermuda and the nearby hydrographic station (Stn S) to assess the utility of this species as a recorder of NAO-related SST variability. Young colonies were used for this calibration exercise, the growth period of which overlaps with the time period covered by the instrumental record. We examined the skeletal architecture at both meso- and ultrastructural levels and conducted an *in situ* field staining experiment over a period of 1 yr to further our understanding of the relationship between skeletal construction and growth and the nature of the proxy record.

MATERIALS AND METHODS

Live colonies of *Diploria labyrinthiformis*, 180 mm to 200 mm in height, were collected at 13 m depth about 1 km from the shore of John Smith's Bay on the south-east edge of the Bermuda platform. Slices (6 mm thick) were cut from the colony centers using a water-cooled tile saw. Petrographic thin sections were made from subsamples of these slices (40 × 25 mm), set in epoxy resin, ground and polished using a series of grit sizes up to 0.1 μm in a diamond suspension. The polished side of the embedded slice was glued to a standard glass petrographic slide and its thickness reduced to 15 μm . An Olympus BHSP polarizing microscope fitted with a PM-10M photomicrographic system camera was used to examine and photograph the skeletal ultrastructure.

X-radiographs of each slice were made at the local hospital with machine settings of 50 kV and 1.6 mAs, a film-focus distance of 1 m and an exposure time of 0.2 s. Based on information about growth rate and life history obtained from the X-radiographs, appropriate slabs were chosen for $\delta^{18}\text{O}$, Sr/Ca and density analyses. We used ScionImage (= National Institute of Health [NIH] image) to assign gray-scale values (intensity units) to scanned X-ray positives and construct the density profiles. We did not attempt to correct for the heel effect (a non-uniformity of an X-ray beam across the diameter of the cone of radiation; Chalker et al. 1985); however, we utilized a long film-focus distance which, combined with the small size of our samples, was intended to minimize the heel effect by utilizing the central beam area where intensity is uniform.

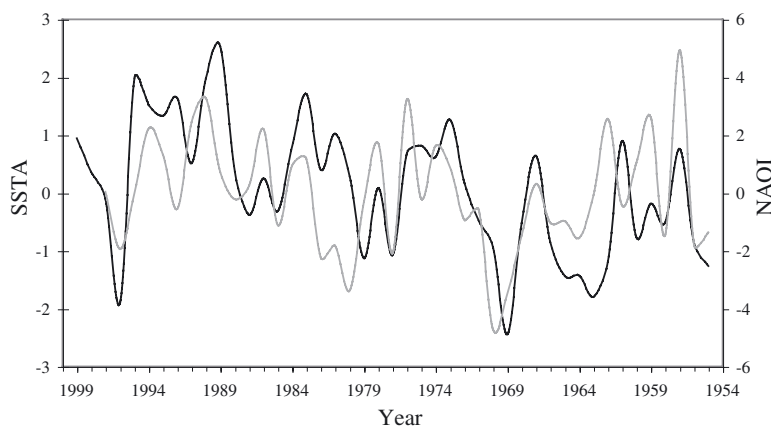


Fig. 1. The North Atlantic Oscillation Index (NAOI, black line) versus averaged wintertime (December–March) sea surface temperature anomalies (SSTA) between 1 and 20 m depth (gray line), 1955 to 1998. SST data available at www.bbsr.edu/cintoo/cintoo.html; NAOI data from Hurrell (1995). Coherency between the records is high ($r_{xy}^2 = 0.99$, zero significance level, $zsl = 0.45$) with stable phase at periods centered on 10 to 11 yr

A 120 mm, 40 yr long $\delta^{18}\text{O}$ profile was constructed from a colony with average growth rate of 3 mm yr^{-1} . The base of the colony had been bored into by mollusks and was not sampled. Subsamples were removed from the theca at 0.2 mm intervals using a hand-held Mini-craft MB170 dental drill fitted with diamond-tipped tapering drill bit. We targeted a single skeletal element to minimize the combination of skeleton of different ages into a single sub-sample. $\delta^{18}\text{O}$ was measured with a VG PRISM stable isotope ratio mass spectrometer fitted with automated 40-sample carousel and common acid bath. More details of the sampling and analysis techniques for coral $\delta^{18}\text{O}$ are given in Cohen & Hart (1997); measurement precision on replicate $\delta^{18}\text{O}$ analyses of the limestone standard NBS-19 was typically 0.03‰.

Microscale measurements of skeletal Sr/Ca ratios were made using a Cameca 3f ion microprobe employing Secondary Ion Mass Spectrometric (SIMS)¹ techniques. The ion microprobe enables *in situ* elemental analyses of intact coral skeleton to be made at micron-scale resolution by targeting discrete crystal bundles within skeletal elements of the corallite. In this study we used a 5 nA O^- beam to sputter the surface of mounted polished sections of *Diploria labyrinthiformis* skeleton. Routine instrument precision for Sr/Ca analyses is 0.3% (2σ). Sample spots of 20 μm diameter were analyzed at 100 μm intervals. To avoid thickening deposits, a sample track was followed close to centers of calcification down the length of the septum (see Fig. 3B). Details of the SIMS measurement technique and its application to coral skeletons is given in Hart & Cohen (1996) and Cohen et al. (2001).

Daily SSTs at John Smith's Bay between 1997 and 2000 were recorded by *in situ* Onset Stowaway XTI temperature data loggers placed at 13 m depth. We used this record to derive equations for the relationships between temperature and $\delta^{18}\text{O}$, and temperature and Sr/Ca. The 45 yr long record of SST at Hydrographic Station S was used to assess the fidelity of the longer coral proxy record. Hydrostation S is an open-ocean site located 15 nautical miles to the south-east of the Bermuda platform at $32^\circ 10' \text{ N}$, $64^\circ 30' \text{ W}$; hydrographic measurements have been quasi-biweekly since 1954. The annual temperature range in the reef (19.4 to 28.4°C) and offshore records (19.5 to 28.0°C) are equivalent; however, a statistical comparison of interannual variability was not possible given the different durations of each record.

Correlations between the North Atlantic Oscillation Index (NAOI) and SST were assessed by estimating the coherence spectrum (Bendat & Piersol 2000), which quantifies correlation as a function of periodicity. Spectral estimates for coherence analysis were made using the overlapping segment method, which reduces uncertainty by averaging the spectra of adjacent blocks of data (Percival & Walden 1993). The same method was used to assess coherence amongst instrumental records and coral proxy data generated in this study.

Seasonality of coral growth was assessed by periodic staining of colonies with sodium alizarin sulphate over a period of 1 yr. An additional 4 live colonies (~50 mm in height) were collected from the study site off John Smith's Bay in June 2000 and placed in shaded, aerated flow-through seawater aquaria for 2 d. The stain (15 mg l^{-1}) was introduced to the aquaria for 24 h, flushed, and the corals allowed to recover for 2 d. They were then returned to the study site and re-attached to the substratum with an underwater cement (7:1 mixture of Portland Type II cement and plaster of paris). The colonies were stained again on September 18, 2000 and January 24, 2001 and collected on June 1, 2001.

RESULTS

Mesoarchitecture

The skeleton of *Diploria labyrinthiformis* comprises a complex arrangement of vertical and horizontal elements (Fig. 2A–C). *D. labyrinthiformis* colonies have elongated, meandering calices (C in Fig. 2A), each containing multiple polyp mouths enclosed by the thecal wall (T in Fig. 2A,B). In *D. labyrinthiformis*, adjacent calices are not contiguous as they are in *Porites* spp., but are separated by an arrangement of skeletal elements collectively referred to as the coenosteum. The theca is cross-cut by numerous vertical plates, called septa (S in Fig. 2C) (Wells 1956), extensions of which form a delicate scaffolding of tangled, vertical pali at the center of the calice. Also within the theca are thin horizontal sheets called dissepiments, laid down at regular intervals to isolate regions of skeleton no longer occupied by tissue. The septa also extend outside the enclosed thecal wall and into the coenosteum as costae (see Fig. 4). The horizontal sheets, or synapticalae, connecting adjacent costae are not true dissepiments. They are substantially thicker with a different arrangement of crystals (i.e. a different ultrastructure). In *D. labyrinthiformis*, the coenosteum is deeply grooved. This groove, called the ambulacrum (AM in Fig. 2A,B), distinguishes *D. labyrinthiformis* from 2 other *Diploria* species, *D. clivosa* and *D.*

¹The Secondary Ion Mass Spectrometer (SIMS) ion microprobe employs a high-energy primary beam of O^- or Cs^+ ions to dislodge atoms from the surface of a material. This process is called sputtering. The dislodged atoms are ionized, separated by mass and counted in a spectrometer. The dislodged atoms represent the secondary ion beam

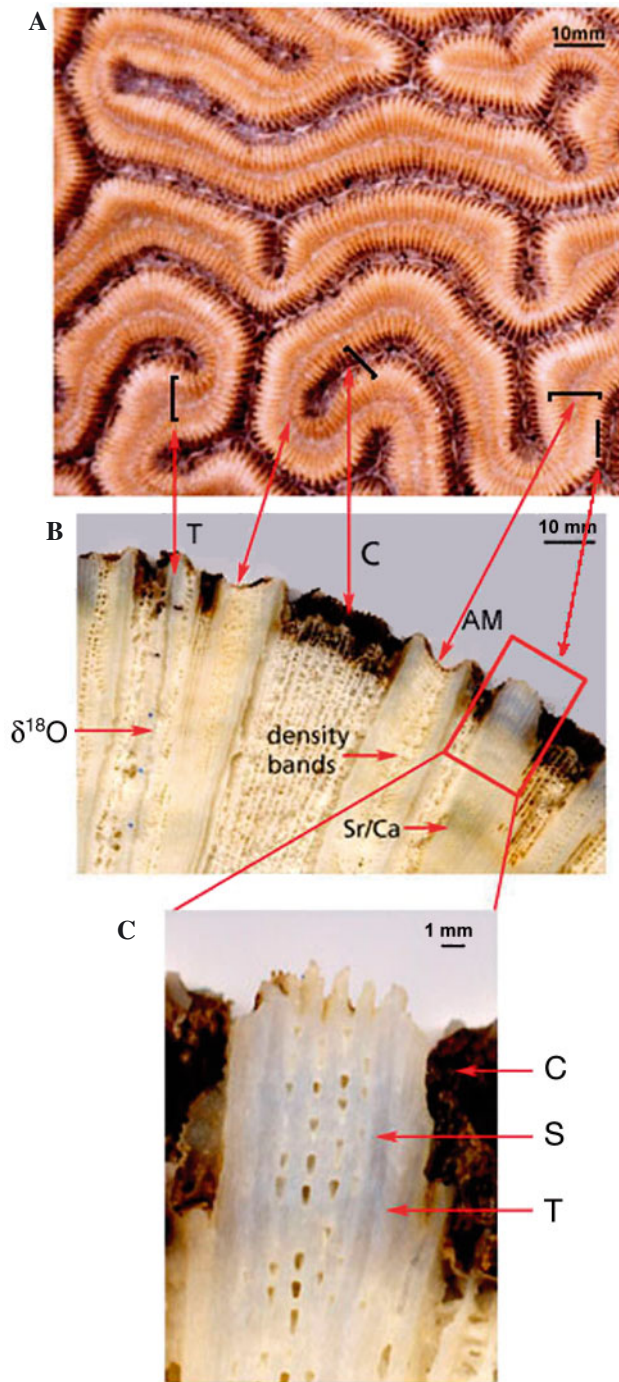


Fig. 2. *Diploria labyrinthiformis*. Mesoarchitecture of skeleton. (A) The surface topography is defined by elongate coralites arranged in longitudinal series; calyx (C) walls are elevated thecae (T) separated from adjacent walls by the ambulacrum (AM); red arrow tips point to precise regions of skeleton; black bars indicate angle of the cut which exposed skeletal elements in (B). (B) Arrangement of skeletal elements and locations of time series measurements in a slab cut from a colony center. The groove drilled for $\delta^{18}\text{O}$ samples is indicated, as is location of density profiles and ion microprobe (Sr/Ca) analyses. (C) Section intercepts the calyx wall in transverse section showing alternating arrangement of translucent septa (S) and opaque thecae (T)

strigosa. In life the ambulacrum contains a gastrovascular canal that connects all polyps and serves to distribute nutrients and respiratory gases throughout the colony (E. Gladfelter pers. comm. 2000).

Skeletal ultrastructure and microbanding

The sclerodermite, the basic unit of coral skeletal microstructure, comprises a center of calcification from which radiate bundles of acicular aragonite crystals (Fig. 3) (Wells 1956). In *Diploria labyrinthiformis*, the theca (T in Fig. 3A) is formed by outgrowths of the sclerodermites of adjacent septa (S in Fig. 3A) and is, strictly speaking, a septotheca (Wells 1956). However, crystal growth from the septa into the theca is discontinuous, as indicated by a clear boundary between the 2 structures (B in Fig. 3A).

In a thick polished section through the thecal wall, the septa appear translucent whereas the theca is opaque (Fig. 2C). The origin of these textural differences are the dark brown microbands visible at centers of calcification and in the acicular crystal bundles of septa and thecae where they are most prominent (Fig. 3B,C). Microbands at the centers of calcification are oriented at right angles to the axis of skeletal extension, indicating that these crystals grow upward from centers of calcification and contribute to the upward growth of the skeletal element (Fig. 3B). Here, the microbands are 9 μm apart on average, and the distance between them is likely to represent growth over a day (Risk & Pearce 1992, Cohen et al. 2001). Microbands in the acicular bundles of the septa and theca are about 2 μm apart and run parallel to the axis of extension. Their orientation indicates that the acicular crystal bundles contribute to the outward growth, or thickening of the septa and theca. The occurrence of many microbands in the crystal bundles suggests that the septa continue to thicken for some time after the original skeletal deposit is made. Assuming that the distance between successive microbands represents daily growth, the number of days over which thickening occurs can be estimated. The entire length of each bundle, from their appearance at the center of the septa to their occlusion at the center of the theca, averages about 400 μm (Fig. 3A). At a growth rate of 2 $\mu\text{m d}^{-1}$, subsurface skeletal thickening, which includes growth of the theca, must continue over a period of about 200 d (6 mo).

Staining experiment

The stained *Diploria labyrinthiformis* colonies were removed on June 1, 2001 and a 5 mm thick section cut

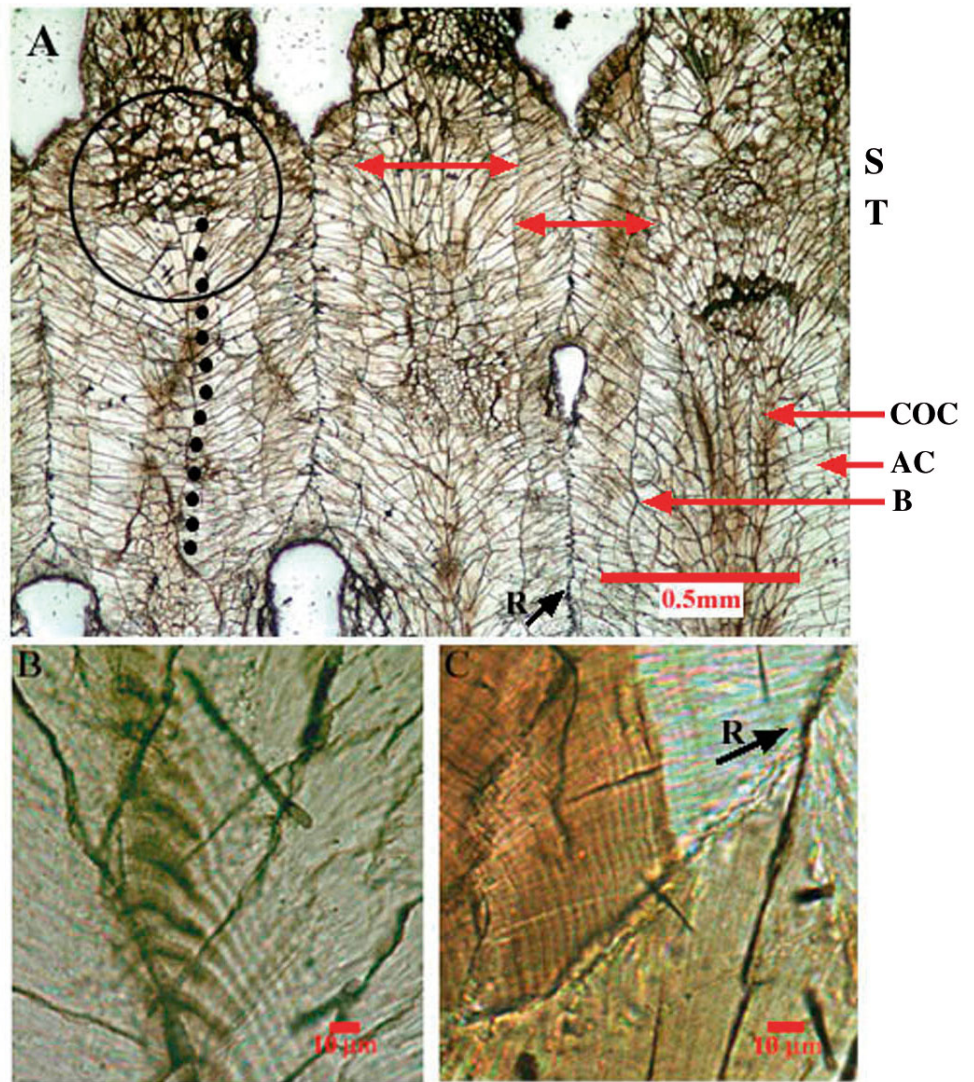
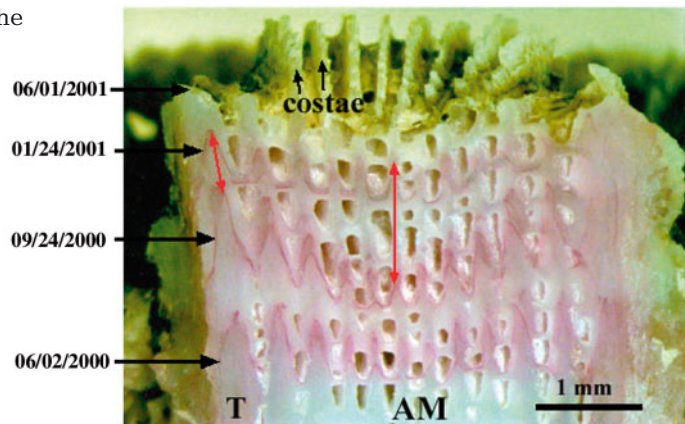


Fig. 3. *Diploria labyrinthiformis*. Skeletal ultrastructure seen in a 15 μm thick petrographic section of the theca. (A) Discrete elevated septal columns (S; upper double-headed arrow) are comprised of centers of calcification (COC) and their associated bundles of acicular crystals (AC); these bundles in the septa are bounded by a growth disruption (B) of unknown duration, whereafter growth resumes to form the theca (T; lower double-headed arrow); bundles from adjacent septa meet and occlude each other, forming an obvious ridge (R). The Sr/Ca time series was constructed from measurements down the center of the septum close to centers of calcification; ion microprobe sample spots are indicated by the vertical line of discrete black circles. For comparison, an area of skeleton extracted by a small dental drill is approximately encircled. (B) Microbands at centers of calcification. (C) Microscale growth bands in the acicular bundles of the theca. Orientation of the bands relative to the growth axis of the colony is perpendicular in (B) and almost parallel in (C)

from the center of each colony. Two colonies had sufficient new growth to reveal 3 discrete, narrow stain lines under a binocular microscope at $5\times$ magnification (Fig. 4). In both colonies, the distance between the lines differed, indicating seasonal variations in skeletal extension rate. Moreover, different regions of the

corallite exhibited different seasonal growth patterns. Skeletal elements in the ambulacrum extended further between late September and late January, a period of cooler water temperatures on Bermuda. Only 25% of

Fig. 4. *Diploria labyrinthiformis*. Discrete Alizarin Red-S stain introduced to living colonies at the collection site during 2000–2001 field season (dates are mo/d/yr). The stain lines reveal seasonality as well as variability in extension rates across the corallite. Skeletal elements in the ambulacrum (AM in Fig. 2) are the costae, which extended most rapidly between late September and later January. Skeletal elements in the thecal wall (T, see also Figs. 2A,C) are the septa and theca, which grew most rapidly in the summer months from June through end of September



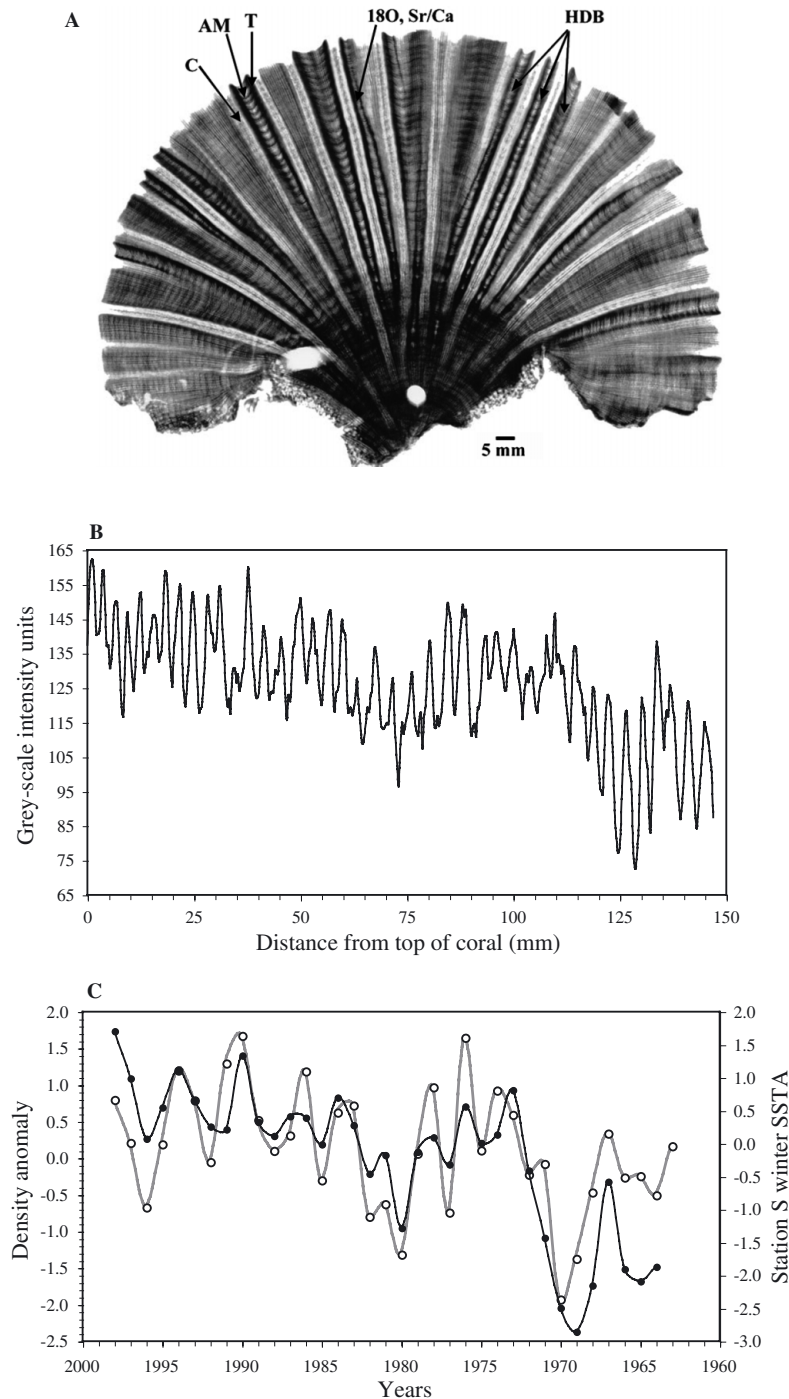


Fig. 5. *Diploria labyrinthiformis*. (A) X-ray positive image showing skeletal density variations. C: calyx, AM: ambulacrum, T: thecal wall, HDB: high-density band. The base of this colony is occupied by anomalously high-density skeleton not seen in the other colonies, which we attributed to biological rather than environmental factors. (B) Annual cycles in skeletal density of the ambulacrum from 1964 to 1998 are resolved from the X-ray positive using NIH-image. (C) Annual wintertime density anomaly (●) is compared with annual wintertime (December–March) SST anomaly in the Stn S hydrographic record for the corresponding time period (○). Intensity units are measured in 0.4 mm intervals

the annual extension in this region of the skeleton occurred during the summer months of June through September. In contrast, septa and thecae extended most rapidly during the warm summer months. Here, more than 50% of the annual skeletal extension occurred between the first 2 staining sessions (June and September). The stain lines also showed that the depth of the ambulacrum changes through the year, increasing during the summer when extension rates along the ridge wall outpaced extension rates in the ambulacral groove, and decreasing in the winter when the opposite trends occurred.

X-ray imaging

Variations in skeletal density occurred across the width and down the length of the colonies (Fig. 5A). Cross-colony variability related to skeletal architecture: low-density regions were the centers of calices, which contained little more than a porous framework of dissepiments and pali; highest-density regions were the thecae. An equivalent percentage change in density occurred down the length of the colonies, in well-defined annual growth bands spaced at intervals of 2 to 4 mm. Annual banding was strongest in the ambulacrum, where the high-density band contributed about 25% of the width of each couplet. Density variations in the ambulacrum corresponded to changes in the size of pores in the lattice of vertical costae and horizontal synapticulae (Fig. 4). Low-density skeleton occurred where the pore spaces were larger and more elongate, between stain lines introduced in late September and late January, i.e. during the cool season (Fig. 4).

The distance between consecutive bands revealed an average growth rate of $3 \pm 0.5 \text{ mm yr}^{-1}$. To generate the density profile in Fig. 5B, we chose a colony whose X-radiograph revealed no dramatic changes in skeletal density over its life history that would mask the climate signal. The profile revealed 35 high-frequency (annual) oscillations superimposed upon longer-term (decadal-scale) changes. Each annual cycle was matched to 1 high–low density band couplet seen in the X-radiograph of this

colony (not shown). In Fig. 5C, the annual wintertime density anomaly was plotted against the annual wintertime SST anomaly recorded at Stn S for the corresponding years. The annual wintertime density anomaly (or standardized departure) is calculated as the difference between the wintertime (lowest) intensity value in each annual cycle and the mean of all wintertime values in all the cycles, divided by the standard deviation of the mean. Coherency between wintertime SSTAs and the annual wintertime coral density anomaly was high, with a stable phase at periods of 2.5 yr ($\hat{\gamma}_{xy}^2 = 0.60$, zero significance level, $zsl = 0.2$) and 10 yr ($\hat{\gamma}_{xy}^2 = 0.60$, $zsl = 0.2$), where $\hat{\gamma}_{xy}^2$ is coherence between $x =$ wintertime coral density and $y =$ wintertime SSTAs; $zsl =$ zero significance level).

Stable Isotope Ratio Analysis (SIRA)

A section of the $\delta^{18}\text{O}$ and corresponding density profiles from a single colony are superimposed in Fig. 6A. The profiles are aligned according to the distance from the surface of the colony. Seasonal high temperatures (low $\delta^{18}\text{O}$) corresponded to seasonal high-density bands and vice versa (Fig. 5B). The full $\delta^{18}\text{O}$ profile is plotted against SSTs recorded at Stn S in Fig. 6B. Given the inverse correlation between coral $\delta^{18}\text{O}$ and SST, we assume that the most recent wintertime $\delta^{18}\text{O}$ value (-2.60‰) reflects the coolest period of the winter prior to collection, i.e. February–March 1999. Note that the amplitude of the latest 2 $\delta^{18}\text{O}$ cycles is almost double that of the preceding cycles. The slope of the $\delta^{18}\text{O}$ –SST regression equation based on the first 2 annual $\delta^{18}\text{O}$ cycles (years 1997 and 1998) and corresponding *in situ* recorded SSTs was $-0.23\text{‰ }^\circ\text{C}^{-1}$, close to the expected value of $0.22\text{‰ }^\circ\text{C}^{-1}$ for marine skeletons (Epstein et al. 1951). However, application of this paleotemperature scale to the remainder of the $\delta^{18}\text{O}$ record (Fig. 6B) yields derived annual SST cycles that were smaller than expected for this site, and the mismatch was most striking in the summertime. The slope of the $\delta^{18}\text{O}$ –SST regression equation based on the first 38 cycles in the 40 yr record ($-0.113\text{‰ }^\circ\text{C}^{-1}$) is half that obtained for the top 2 (most recent) cycles (Fig. 6B).

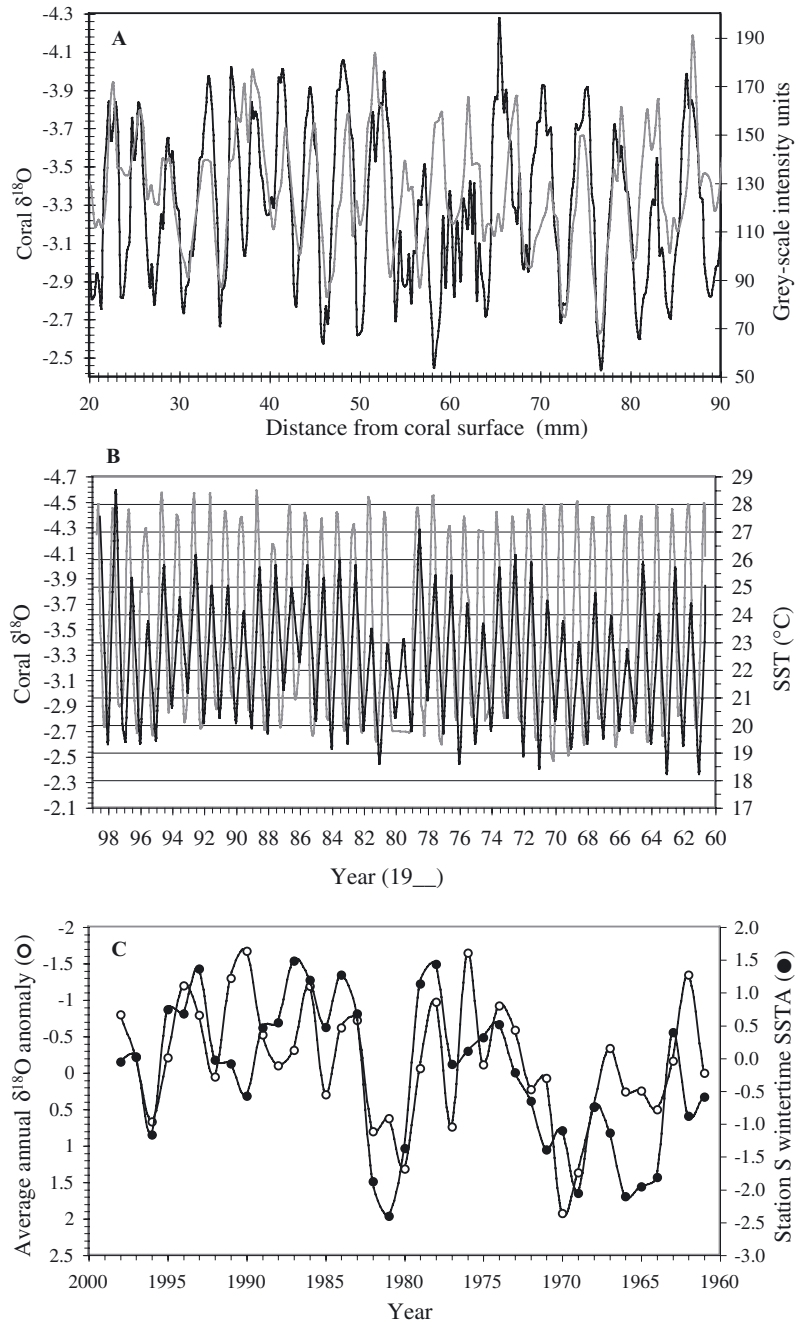


Fig. 6. *Diploria labyrinthiformis*. (A) Oxygen isotope ratios (black line) compared with a seasonally resolved density profile of the same colony constructed using NIH-Image (gray line). (B) Stn S SSTs (gray line) plotted against seasonally resolved $\delta^{18}\text{O}$ profile (black line) for the years 1960 through 1998 ($R^2 = 0.68$, slope = -0.1123). (C) Stn S wintertime SSTAs (O); oxygen isotope abnormalities (●). Time period covered by plot is summer of 1961 through summer of 1998

The annual $\delta^{18}\text{O}$ anomaly was compared with annual wintertime SST anomaly in the Stn S time series between 1960 and 1998 (Fig. 6C). The $\delta^{18}\text{O}$ anomaly for a specific year was calculated as the difference between the average annual $\delta^{18}\text{O}$ of that

year and the mean of all annual $\delta^{18}\text{O}$ values in all the years, divided by the standard deviation of the mean. Coherency between the records is high, with a stable phase at periods centered on 10 yr ($\hat{\gamma}_{xy}^2 = 0.60$, $\text{zsl} = 0.2$).

SIMS microscale analysis of Sr/Ca

A 17.5 mm long SIMS-generated Sr/Ca profile is shown in Fig. 7A. In the time series, 7 distinct annual Sr/Ca cycles are seen, with an average amplitude of 0.8 mmol/mol. At 0.95 mm down from the tip of the septum, i.e. during the early summer of 1995, we made 11 Sr/Ca measurements across its width and into the adjacent thecae, a total distance of 400 μm (Fig. 7A). The range of values in the horizontal profile, excluding the center of calcification, was 1 mmol/mol, which is

greater than the annual average cycle in Sr/Ca and equal to the range of Sr/Ca values obtained throughout the year 1995.

The annual range of *in situ* logged SSTs at the collection site, averaged at biweekly intervals, was 10°C. Using these data, we calculated the slope of the Sr/Ca-SST regression equation by comparing annual maximum and minimum Sr/Ca values with corresponding maxima and minima in SST. The slope, -0.0843 mmol/mol °C⁻¹, was close to that obtained for Hawaiian *Porites* spp. corals (-0.0795 mmol/mol °C⁻¹) (de Villiers et al. 1994) but twice as steep as that obtained for Bermuda *Diploria labyrinthiformis* using bulk sampling techniques (Cardinal et al. 2000).

The average annual wintertime Sr/Ca-derived SST anomalies were calculated using the Sr/Ca-SST equation derived from seasonal data, and compared with annual average wintertime SSTAs from the Stn S time series between 1992 and 1999 (Fig. 7B). In general, the interannual SST variability recorded at Stn S was reflected by the coral Sr/Ca ($R^2 = 0.77$). However, the 1995/1996 SST cool-water anomaly (associated with a negative NAOI) of 1°C was exaggerated by the coral Sr/Ca thermometer, which indicated an anomaly of double that magnitude.

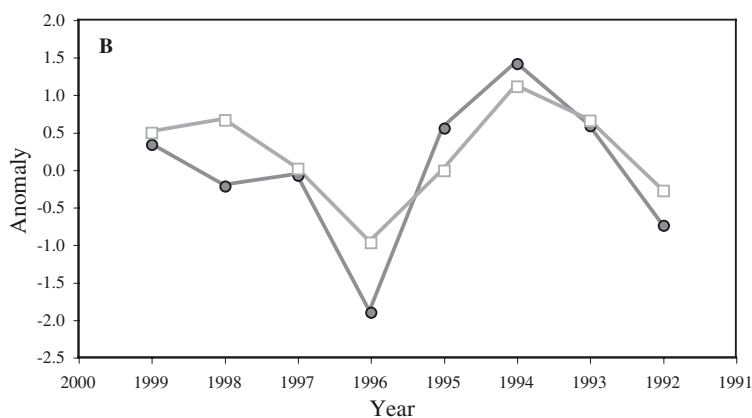
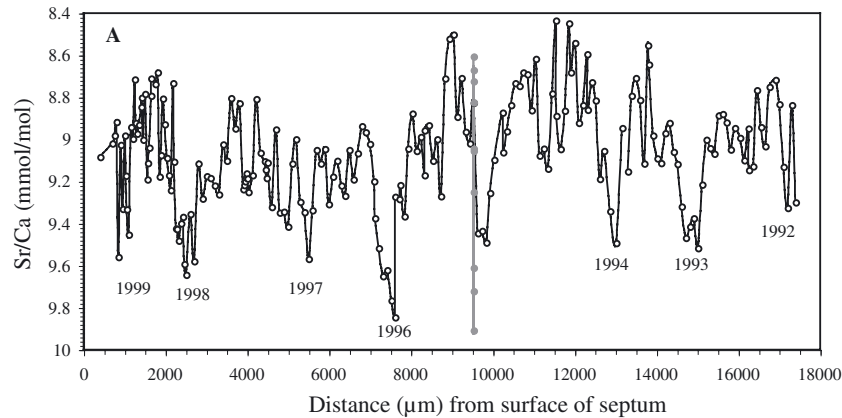


Fig. 7. *Diploria labyrinthiformis*. (A) Strontium/calcium (Sr/Ca) time series generated using SIMS (secondary ion mass spectrometer) ion microprobe, spanning the time period 1992 through 1999 (○). A horizontal profile was generated across the width of the septum and into the theca at the start of summer 1995 (●). The spread of values across the septum in the summertime is equivalent to a full annual Sr/Ca cycle, suggesting that the original summertime deposition is thickened with fall and wintertime deposits through 1996. (B) Averaged wintertime Sr/Ca values from each Sr/Ca cycle (●) are compared with annual NAOI and annual wintertime Stn S SSTs (□) from 1992 to 1999

DISCUSSION

Colony architecture, ultrastructure and growth

Examination of skeletal meso- and ultrastructure of *Diploria labyrinthiformis*, combined with information about skeletal growth gained from *in situ* staining of live colonies and the X-radiographs, revealed characteristics peculiar to this species that have implications for the nature and temporal resolution of proxy records obtained using different sampling techniques. Despite the apparent high sampling resolution, bulk sampling techniques such as that used by Cardinal et al. (2000) combine different skeletal elements of different ages into a single sample. The upper margins of septa are about 5 mm above the bottoms of calices, equivalent to about 2 yr of growth of a *D. labyrinthiformis* colony on Bermuda's south-shore reefs. A sample removed across the calice will average skeleton grown over 2 yr and will not resolve the

seasonal or interannual variability. The tips of the septa rise about 1 mm above the tips of the thecae (Fig. 2C). Therefore, the subsampling technique employed by Cardinal et al. (2000) which crosscuts the thecal wall (see our Fig. 2) combines skeleton accreted over a full year and cannot resolve monthly variability.

The presence of microbands in the septa and theca, oriented parallel to the upward growth axis of the colony, suggests that the septa continue to thicken over a period of time after the original material is laid down, i.e. for as long as the skeleton is in contact with live tissue. Indeed, growth of the theca itself is a product of thickening of the septa, facilitated by the presence of tissue in the grooves between adjacent septa. The number of fine bands seen in the thin section as well as the depth of the tissue layer in the calyx (3 to 4 mm, see Fig. 2B) indicate that bulk skeletal samples removed from the calyx or the surrounding theca are likely to include thickening deposits representing growth over more than a year.

In situ staining revealed seasonal differences in the extension rate of skeletal elements in the calice compared with those of the ambulacrum. Seasonally resolved time series constructed from the costae will appear biased toward the cool season, with extended wintertime peaks and narrow summertime peaks in the annual cycle. On the contrary, time series constructed along septa and thecae will reflect largely summertime values with extended summertime peaks and narrow wintertime peaks in the annual cycle. These observations may explain the variations observed amongst proxy time series constructed from *Diploria labyrinthiformis* colonies reported by Cardinal et al. (2000).

Skeletal density

High- and lower-frequency changes in skeletal density are seen in X-radiographs of *Diploria labyrinthiformis* skeleton. The former are the annual growth bands, characteristic of all massive reef species. In *D. labyrinthiformis*, the bands are strongest in the ambulacrum, which might explain the lack of well-defined density banding in *Diploria* species in which the ambulacrum is either absent (*D. clivosa*) or shallow (*D. strigosa*). The structural basis for the density banding in *D. labyrinthiformis* appears to be changes in the size of pore spaces (alternatively, the thickness of skeletal elements—costae and synapticulae) in the ambulacrum. Dodge et al. (1993) provided a similar explanation for density variations in *Montastrea annularis*, a species whose skeletal architecture is similar in that adjacent polyps are separated by exothecal structures. The relationship between pore-size distribution and the stain

lines indicates that the wider, low-density portion of the density-band couplet in the ambulacrum forms in the wintertime, whereas the narrow high-density skeleton appears to be formed in the summer. This observation is supported by the phase correspondence between high- (low-) density skeleton and low or more negative (enriched) $\delta^{18}\text{O}$ (Fig. 6A), which suggests that a large proportion of the high density skeleton in *D. labyrinthiformis* is accreted during the warm season.

Skeletal density also exhibits significant variability on interannual and decadal timescales. In particular, changes in the density of ambulacral skeleton accreted during the wintertime is strongly correlated with changes in wintertime SSTs recorded at Stn S (Fig. 5C). In general, periods of high skeletal density correspond with periods of warm winter SSTs and vice versa, in agreement with the apparent seasonality of density-band formation. Most notably, skeletal density tracks low SSTs in the late 1960s, the subsequent high of the early 1970s and the decadal oscillations superimposed upon a general rise in SSTs over the subsequent 25 yr.

The mechanism linking skeletal density of Bermuda *Diploria labyrinthiformis* with temperature has not been determined in this study. Lough & Barnes (1997, 2000) demonstrated the linear relationship between calcification rate of *Porites* spp. and Great Barrier Reef SSTs over a temperature range of 18 through 29°C. A correlation between skeletal density in *D. labyrinthiformis* and temperatures on Bermuda's northern reefs has also been reported by Draschba et al. (2000). An inverse correlation between skeletal extension and temperature was also noted by Dodge & Vaisnys (1975) for *D. strigosa* and J. Patzold for *Montastrea annularis* (in Dunbar & Cole 1993). We propose that the observed correlations amongst skeletal density, skeletal extension and temperature may be a function of tissue growth rather than calcification rate of the skeleton. How much the coral skeleton extends upward depends on the thickness of the coral tissue layer. In Bermuda, the nutrients that feed tissue growth are highest in the mixed layer during winter. This promotes growth of coral tissue, resulting in a thicker tissue layer and a wider low density band of skeleton. In colder-than-normal years that have deeper winter mixed layers (a typically negative NAO index), even more dissolved inorganic carbon (DIC) and more nutrients are brought to the upper ocean (Gruber et al. 2002). Thus, the effect of nutrients to increase tissue growth and decrease skeletal density is enhanced. The opposite occurs in summer, when fewer nutrients in the shallow mixed layer retard tissue growth, resulting in a thinner tissue layer. The same amount of aragonite (calcification) may be produced (or more due to warmer waters) but is spread over a thinner band of tissue. The result is proportionately higher density skeleton for that sea-

son. The effect is exaggerated during warmer-than-normal summers (typically positive NAO index).

$\delta^{18}\text{O}$

The effects of skeletal thickening on the resolution of the proxy record are most obvious in the $\delta^{18}\text{O}$ profile generated by bulk sampling. We addressed the limitations imposed by slow growth rate and convoluted topography by adopting a sampling resolution of 0.2 mm (<1 mo) and restricting sampling to the thecal element. Although this approach succeeded in generating clear annual cycles in $\delta^{18}\text{O}$, those beneath the tissue layer (i.e. excepting the last 2 yr of the record) did not capture the full amplitude of the annual SST cycle. Indeed, the slope of the $\delta^{18}\text{O}$ -SST regression equation ($-0.113\text{‰ }^{\circ}\text{C}^{-1}$), which is close to the value ($-0.129\text{‰ }^{\circ}\text{C}^{-1}$) obtained by Cardinal et al. (2000) for *Diploria labyrinthiformis* from Bermuda, is significantly lower than the expected $\delta^{18}\text{O}$ -SST slope of $-0.22\text{‰ }^{\circ}\text{C}^{-1}$. It predicts an annual range of SST variability at Bermuda of about 5.5°C , which is 2.5°C short of the true range.

Although coral $\delta^{18}\text{O}$ is a function of both temperature and $\delta^{18}\text{O}_{\text{SEAWATER}}$, the origins of this discrepancy are unlikely to be caused by seasonal variations in $\delta^{18}\text{O}_{\text{SEAWATER}}$, which can be calculated from known changes in salinity. The seasonal range of salinity on Bermuda is about 0.3‰, equivalent to a $\delta^{18}\text{O}$ -derived temperature change of 0.2 to 0.3°C . This is unlikely to account for the shallow gradient of the $\delta^{18}\text{O}$ -SST regression. A more plausible explanation is the effect of skeletal thickening, whereby, at any level in a vertical skeletal element, the skeleton comprises the initial deposition that lengthened the skeletal element plus the subsequent growth that thickened it (Barnes et al. 1995). According to this model, the initial deposition represents skeletal growth over a few days or weeks while the thickening process continues over months or years for as long as the skeletal element is in contact with living tissue. The implication of skeletal thickening for the *Diploria labyrinthiformis* $\delta^{18}\text{O}$ record is that the original summertime deposits, thickened during the fall and wintertime, will have heavier (more positive) $\delta^{18}\text{O}$ values than expected. This is what we observed, at least for skeleton that had already been vacated by living tissue (i.e. the first 38 $\delta^{18}\text{O}$ cycles). The presence of microbanding in the septa and theca, and the relative narrowness of pore spaces in ambulacral skeleton enclosed by summertime stain lines, supports the hypothesis that summertime skeleton in *D. labyrinthiformis* continues to thicken over a period of time. We do not yet have sufficient data to calculate the exact contribution of each season's growth to the bulk of the high-density band.

There is a strong correlation between the average annual $\delta^{18}\text{O}$ anomaly and the recorded wintertime SST anomaly. This suggests an overrepresentation of wintertime information by the coral skeleton and may indicate that a large proportion of the high-density band is contributed by the wintertime thickening deposits. Indeed, despite the thickening problem, coral-derived SSTs track low-frequency wintertime variability indicated by the instrumental record for much of the 40 yr time period, notably the warmth of the early 1960s, the mid-60s cooling and subsequent rapid warming which peaked in the mid-1970s (Fig. 6C). Thus, although $\delta^{18}\text{O}$ profiles generated from bulk samples of *Diploria labyrinthiformis* skeleton are not of sufficiently high resolution to capture the full annual temperature range, much of the low-frequency (decadal scale) wintertime SST variability was captured in the record.

Sr/Ca

The Sr/Ca profile generated across the width of the septum provides further evidence that summertime skeleton is thickened by subsequent fall and wintertime deposits (Fig. 7A). Sr/Ca values at the start of the horizontal profile, i.e. at the center of the septum, indicate that skeleton accreted during the early summer of 1995. Toward the outer edges of the septum however, in the same horizontal plane, the horizontal profile captured high Sr/Ca values equivalent to those seen in the following (1995–1996) winter. We interpret these results to indicate that acicular crystals in the septa that started growth in the summertime of 1995 continued to grow outward (thicken) through the following winter of 1995–1996, in agreement with the skeletal thickening hypothesis proposed by Barnes & Lough (1993). The implications are that bulk sampling techniques, which do not distinguish between microscale regions of coral skeleton, will not produce seasonally or annually resolved time series from this species (see also Barnes et al. 1995).

Using the microscale sampling technique, we avoided the thickening deposits, and generated a Sr/Ca time series that captured the full amplitude of the annual SST cycle. The slope of the Sr/Ca–SST regression equation obtained here for *Diploria labyrinthiformis*, $-0.0843\text{ mmol/mol }^{\circ}\text{C}^{-1}$, is close to that obtained for Hawaiian *Porites* corals ($-0.0795\text{ mmol/mol }^{\circ}\text{C}^{-1}$; de Villiers et al. 1994). Our data suggest that the temperature sensitivity of Sr in the daytime skeleton of *Diploria* aragonite may be equivalent to that in fast-growing tropical reef corals, contrary to the interpretation by Cardinal et al. (2000) based on TIMS (Thermal Ionization Mass Spectrometry) Sr/Ca analysis of bulk skeletal samples. The slope of the

Sr/Ca–SST equation calculated from Cardinal et al.'s study ($-0.045 \text{ mmol/mol } ^\circ\text{C}^{-1}$) is half that of the slope obtained in this study. We propose that the Sr/Ca–SST regression produced by bulk sampling is, as observed with our $\delta^{18}\text{O}$ data, an inaccurate representation of the actual slope. The amplitude of the annual Sr/Ca and $\delta^{18}\text{O}$ cycles generated from bulk, rather than microscale, samples are dampened because bulk sampling techniques cannot distinguish between initial skeletal deposits and the thickening deposits. The range of values obtained in the horizontal Sr/Ca profile lends further support to our observation of long-term subsurface skeletal thickening in this species and demonstrates its significance.

The Sr/Ca time series also provides information about skeletal extension along the septum. The average annual extension rate of 2.5 mm indicated by the length of each Sr/Ca cycle in this colony is lower than that estimated from the width of the density bands seen in the x-radiograph and from the width of the annual $\delta^{18}\text{O}$ cycles, both of which indicate an average extension rate closer to 3 mm yr^{-1} . The origin of these differences is unclear but may be caused by variable extension rates of different skeletal elements in the corallite. The asymmetry of the annual Sr/Ca cycles, with wide summer maxima and short sharp winter minima occurs because the extension rates of skeletal elements vary seasonally, and extension rates are highest along the corallite wall during the summer, in agreement with our observations based on *in situ* staining.

The interannual variability in wintertime Sr/Ca agrees well with the interannual variability in recorded wintertime SSTs at Stn S (Fig. 7B) with the exception of the -1°C anomaly in winter 1995–1996 which the coral reads as a -2°C anomaly. Exaggeration of Sr/Ca-derived SSTs by the coral *Porites* spp. has been observed during El Niño- and La Niña-induced SSTAs on the Great Barrier Reef (McCulloch et al. 1994, Marshall 2000), and it is yet unclear why this should occur. Cohen et al. (2001, 2002) suggested that Sr/Ca ratios of coral skeleton accreted in the daytime may be influenced more by skeletal calcification rates than they are by SST, an hypothesis supported by recent experimental data (Ferrier-Pages et al. 2003). If this is true, then the 1995–1996 Sr/Ca anomaly in the brain coral skeleton may reflect a decrease in coral calcification rate in response to the drop in water temperature associated with the unusually low NAOI.

CONCLUSIONS

The skeletal scaffolding of *Diploria labyrinthiformis* is reinforced by thickening of skeletal elements beneath the surface of the colony. Skeletal thickening

may be a seasonal process, with greater thickening of summertime skeleton occurring in winter months. Bulk sampling techniques do not distinguish initial deposits from thickening deposits, and result in reduced amplitude and temporal resolution of proxy data.

Linear extension varies seasonally and amongst different parts of the corallite. Rapid extension of the costae occurs in fall and wintertime, while septa and thecae grow fastest in summer. This offset in seasonal growth patterns between different parts of the corallite implies that geochemical measurements made from different skeletal elements in the corallite will better reflect the climatology of different seasons.

The skeletal density of *Diploria labyrinthiformis* is temperature-sensitive and increases with increasing water temperature. The wintertime skeletal density anomaly is well correlated with the winter SSTA on interannual and decadal timescales. This density-based thermometer is a potentially valuable and inexpensive tool for reconstructing low-frequency SST variability of the western North Atlantic.

The $\delta^{18}\text{O}$ of skeleton beneath the tissue layer, sampled at monthly resolution, does not capture the full amplitude of the seasonal SST cycle. We propose that the $\delta^{18}\text{O}$ of summertime skeleton is heavier than predicted because original summertime deposits are overlain by skeleton accreted during the following fall and wintertime. As a result, the $\delta^{18}\text{O}$ record is biased toward the wintertime.

The Sr/Ca of unthickened skeleton measured with SIMS ion microprobe captures the full amplitude of the seasonal SST cycle. However, the Sr/Ca–SST regression equation derived from seasonal data overestimated the magnitude of the 1995–1996 SST anomaly.

Acknowledgements. The authors are most grateful for the assistance of Graham Webster, the staff and students in the BBSR Benthic Laboratory during coral collection and staining. Ms J. Smith and staff of the X-radiography unit at Falmouth Hospital on Cape Cod, Massachusetts, were exceptionally helpful and accommodating in our unusual task. We thank Mr. A. Gagnon, WHOI NOSAMS facility, for $\delta^{18}\text{O}$ analyses and Dr. G. D. Layne, WHOI Ion Microprobe facility, for assistance with ion microprobe analyses. We are grateful to Dr. R. Sohn (WHOI) who custom-wrote the code for cross-spectral analyses. Staff at National Petrographic Inc. are thanked for preparation of thin sections. Suggestions by 3 anonymous reviewers considerably improved the manuscript. This work was supported by NOAA CLIVAR Atlantic #NA96-GPO461 to A.L.C. and M.S.M. The Bermuda Government provided support to S.R.S. during this study. This is WHOI contribution number 11138.

LITERATURE CITED

Barnes DJ, Lough JM (1993) On the nature and causes of density banding in massive coral skeletons. *J Exp Mar Biol Ecol* 167:91–108

- Barnes DJ, Taylor RB, Lough JM (1995) On the inclusion of trace materials into cycles due to growth processes. *J Exp Mar Biol Ecol* 194:251–275
- Bates NR (2001) Interannual variability of oceanic CO₂ and biogeochemical properties in the Western North Atlantic subtropical gyre. *Deep-Sea Res II* 48:1507–1528
- Bendat JS, Piersol AG (2000) *Random data: analysis and measurement procedures*, 3rd edn. John Wiley & Sons, New York, p 218–252
- Bjerknes J (1964) Atlantic air-sea interaction. *Adv Geophys* 10:1–82
- Cardinal D, Hamelin B, Bard E, Paetzold J (2000) Sr/Ca, U/Ca and δ¹⁸O records in Recent massive corals from Bermuda; relationships with sea surface temperature. *Chem Geol* 176:213–233
- Chalker B, Barnes D, Isdale P (1985) Calibration of X-ray densitometry for the measurement of coral skeletal density. *Coral Reefs* 4:95–100
- Cohen AL, Hart SR (1997) The effect of colony topography on climate signals in coral skeleton. *Geochim Cosmochim Acta* 61:3905–3912
- Cohen AL, Layne GD, Hart SR, Lobel PS (2001) Kinetic control of skeletal Sr/Ca in a symbiotic coral: implications for the paleotemperature proxy. *Paleoceanography* 16:20–26
- Cohen AL, Owens KE, Layne GD, Shimizu N (2002) The effect of algal symbiosis on the accuracy of Sr/Ca paleotemperatures from Coral. *Science* 296:331–333
- Cole JE, Dunbar RB (1999) Annual records of tropical systems: recommendations for research. PAGES Workshop Report Series 99–1, PAGES, Bern
- Cole JE, Fairbanks RG, Shen GT (1993) Recent variability in the Southern Oscillation; isotopic results from a Tarawa Atoll coral. *Science* 260:1790–1793
- de Villiers S, Nelson BK, Chivas AR (1994) The Sr/Ca-temperature relationship in coralline aragonite: influence of variability in (Sr/Ca) seawater and skeletal growth parameters. *Geochim Cosmochim Acta* 58:197–208
- Dodge RE, Thomson J (1974) The natural radiochemical and growth records in contemporary hermatypic corals from the Atlantic and Caribbean. *Earth Planet Sci Lett* 23:313–322
- Dodge RE, Vaisnys JR (1975) Hermatypic coral growth banding as environmental recorder. *Nature* 258:706–708.
- Dodge RE, Szmant AM, Garcia R, Swart PK, Forester A, Leder JJ (1993) Skeletal structural basis of density banding in the reef coral *Montastrea annularis*. *Proc 7th Int Coral Reefs Symp Guam* 1:186–195
- Draschba S, Patzold J, Wefer G (2000) North Atlantic climate variability since AD 1350 recorded in δ¹⁸O and skeletal density of Bermuda corals. *Int J Earth Sci* 88:733–741
- Dunbar RB, Cole JE (1993) Coral records of ocean-atmosphere variability: report from the Workshop on Coral Paleoclimate Reconstruction. NOAA Climate & Global Change Program Special Report No. 10. UCAR, Boulder, CO
- Epstein S, Buchsbaum R, Lowenstam HA, Urey HC (1951) Carbonate-water isotopic temperature scale. *Geol Soc Am Bull* 62 (4):417–425
- Ferrier-Pages C, Boisson F, Allemand D, Tambutte E (2003) Kinetics of strontium uptake in the scleractinian coral *Stylophora pistillata*. *Mar Ecol Prog Ser* 245:93–100
- Gagan MK, Ayliffe LK, Beck JW, Cole JE, Druffel ERM, Dunbar RB, Schrag DP (2000) New views of tropical paleoclimates from corals. In: Alverson KD, Oldfield F, Bradley RS (eds) *Past global changes and their significance for the future*. *Quat Sci Rev* 19:45–64
- Gruber N, Keeling CD, Bates NR (2002) Interannual variability in the North Atlantic Ocean carbon sink. *Science* 298:2374–2378
- Hart SR, Cohen AL (1996) Sr/Ca in corals: an ionprobe study of annual cycles and microscale coherence with other trace elements. *Geochim Cosmochim Acta* 60:3075–3084
- Hurrell JW (1995) Decadal trends in the North Atlantic Oscillation: regional temperatures and precipitation. *Science* 269:676–679
- Joyce TM, Robbins P (1996) The long-term hydrographic record at Bermuda. *J Clim* 9:3121–3131
- Logan A, Tomascik T (1991) Extension growth rates in two coral species from high-latitude reefs of Bermuda. *Coral Reefs* 10:155–160
- Logan A, Tomascik T (1994) Linear extension growth rates in two species of *Diploria* from high-latitude reefs of Bermuda. *Coral Reefs* 13:225–230
- Lough JM, Barnes DJ (1997) Several centuries of variation in skeletal extension density and calcification in massive *Porites* colonies from the Great Barrier Reef: a proxy for seawater temperature and a background of variability against which to identify unnatural change. *J Exp Mar Biol Ecol* 211:29–67
- Lough JM, Barnes DJ (2000) Environmental controls on growth of the massive coral *Porites*. *J Exp Mar Biol Ecol* 245:225–243
- Marshall J (2000) High resolution paleoclimate records in corals. PhD thesis, Australian National University, Canberra
- McCulloch MT, Gagan MK, Mortimer GE, Chivas AR, Isdale PJ (1994) A high-resolution Sr/Ca and ¹⁸O coral record from the Great Barrier Reef, Australia, and the 1982–1983 El Niño. *Geochim Cosmochim Acta* 58:2747–2754
- Molinari RL, Mayer D, Festa J, Bezdek H (1997) Multi-year variability in the near surface temperature structure of the mid-latitude western North Atlantic Ocean. *J Geophys Res* 102:3267–3278
- Percival DB, Walden AT (1993) *Spectral analysis for physical applications: multitaper and conventional univariate techniques*. Cambridge University Press, Cambridge, p 289–294
- Quinn TM, Crowley TJ, Taylor FW, Henin C, Joannot P, Join Y (1998) A multicentury stable isotope record from a New Caledonia coral; interannual and decadal sea surface temperature. *Paleoceanography* 13:412–426
- Risk MJ, Pearce TH (1992) Interference imaging of daily growth bands in massive corals. *Nature* 358:572–573
- Talley LD (1996) North Atlantic circulation and variability reviewed for the CNLS conference. *Physica 's Grav D* 98:625–646
- Urban FE, Cole JE, Overpeck JT (2000) Influence of mean climate change on climate variability from a 155-year tropical Pacific coral record. *Nature* 407:989–993
- Visbeck MH, Hurrell JW, Polvani L, Cullen HM (2001) The North Atlantic Oscillation: past, present and future. *Proc Natl Acad Sci USA* 98:12876–12877
- Wells JW (1956) Scleractinia. In: Moore RC (ed) *Treatise on invertebrate paleontology*, Part F. Geological Society of America, New York, p F328–F444